Analyzing spatial transcriptomics and neuroimaging data in neurodegenerative diseases

Keo, D.

Chapter 2

Cholinergic genes in the healthy brain are differentially expressed in regions that exhibit gray matter loss in Parkinson's disease

Arlin Keo

Oleh Dzyubachyk

Jeroen van der Grond

Anne Hafkemeijer

Wilma D.J. van de Berg

Jacobus J. van Hilten

Marcel J. T. Reinders

Ahmed Mahfouz

This chapter was published online in: *bioRxiv* (2019), doi: 10.1101/2019.12.17.875880
(in submission)
Supplementary material is available online at:
https://www.biorxiv.org/content/10.1101/2019.12.17.875880v1.supplementary-material

Abstract

Structural covariance networks are able to identify functionally organized brain regions by gray matter volume covariance across a population. We examined the transcriptomic signatures of such anatomical networks in the healthy brain using post-mortem microarray data from the Allen Human Brain Atlas. A previous study revealed that a posterior cingulate network and anterior cingulate network showed decreased gray matter in brains of Parkinson's disease patients. Therefore, we examined these two anatomical networks to understand the underlying molecular processes that may be involved in Parkinson's disease. Whole brain transcriptomics from the healthy brain revealed upregulation of genes associated with serotonin, GPCR, GABA, glutamate, and RAS signaling pathways. Our results also suggest involvement of the cholinergic circuit, in which genes *NPPA*, *SOSTDC1*, and *TYRP1* may play a functional role. Finally, both networks were enriched for genes associated with neuropsychiatric disorders that overlap with Parkinson's disease symptoms. The identified genes and pathways contribute to healthy functions of the posterior and anterior cingulate networks and disruptions to these functions may in turn contribute to the pathological and clinical events observed in Parkinson's disease.

2.1 Introduction

Parkinson's disease (PD) is a neurodegenerative disorder characterized by the impairment of diverse motor and non-motor symptoms that get progressively worse over time [1]. The decline in clinical performance has been associated with changes in morphological properties of structural and functional neuroimaging networks [2–4]. In turn, studies have investigated the relationship between imaging networks and genetic risk factors associated with PD to provide new insights into the pathogenesis of PD [5–8]. However, less is known about the functions that underlie the spatial organization of brain regions contributing to PD. To identify the molecular mechanisms underlying changes in structural and functional networks in PD, imaging data has been integrated with brain-wide healthy gene expression from the Allen Human Brain Atlas (AHBA) [9,10]. Regional brain atrophy in PD patients was correlated with the expression of genes implicated in trans-synaptic alpha-synuclein transfer [11] and a loss of regional connectivity in PD patients was correlated with the regional expression of *MAPT* in the healthy brain [12]. These studies showed that combining imaging data in PD and gene expression from the healthy brain can shed light on the molecular mechanisms underlying the morphological differences between PD and controls.

Structural covariance networks (SCNs) identify brain regions that co-vary in gray matter volume across a population and can reveal functional network organizations [13]. SCNs have been shown to be dysregulated in different neurological disorders [14–18], and gray matter variations in SCNs can be explained by transcriptomic similarity and structural connectivity [19,20]. Hafkemeijer *et al.* [21] identified nine SCNs based on gray matter variation among healthy middle-aged to older adults. Gray matter volume in four of these nine networks was negatively associated with age: a subcortical network, sensorimotor network, posterior cingulate networks, and anterior cingulate network. Two of these networks were found to show loss of gray matter volume in PD patients beyond the effects of aging: the posterior cingulate network and anterior cingulate network [2]. Atrophy within these two networks was also associated with cognitive impairment and daytime sleepiness, respectively. Together these studies revealed how brain networks change in aging and PD, but the molecular mechanisms contributing to the relevant SCNs remain unclear.

Here, we investigated the transcriptomic signatures of the anterior and posterior cingulate networks within the healthy brain. By integrating the nine SCNs with spatial gene expression data from the Allen Human Brain Atlas, we showed that genes highly expressed in the posterior and anterior cingulate networks were associated with multiple neurotransmitter signaling pathways as well as with memory-related, pain-related, and neuropsychiatric disorders. In addition, both networks showed high expression of cholinergic marker genes that are known to act as regulators of extracellular signaling. Our results provide new insights into the molecular processes underlying anatomical network function and aids in better understanding the selective progression of PD.

2.2 Materials and Methods

2.2.1 Transcriptomic data preprocessing

To understand transcriptomic signatures of nine anatomical networks of the healthy brain, we analyzed gene expression data from the AHBA, a post-mortem microarray data set of 3,702 anatomical brain regions from six non-neurological individuals (5 males and 1 female, mean age 42, range 24–57 years) [10]. Normalized gene expression from the AHBA was downloaded from http://human.brain-map.org/. To filter and map probes to genes, the data was concatenated across the six donors. We removed 10,521 probes with missing Entrez IDs, and 6,068 probes with low presence as they were expressed above background in <1% of samples (PA-call containing presence/absence flag) [10]. The remaining 44,072 probes were mapped to 20,017 genes with unique Entrez IDs using the *collapseRows*-function in R-package WGCNA v1.64.1 [22] as follows: (i) if there is one probe, that one probe is chosen, (ii) if there are two probes, the one with maximum variance across all samples is chosen (method="maxRowVariance"), (iii) if there are more than two probes, the probe with the highest connectivity (summed adjacency) is chosen (connectivityBasedCollapsing = TRUE).

For visualization of gene expression in heatmaps, data was Z-score normalized across all samples for each brain donor separately. Heatmaps were plotted using R-package ComplexHeatmap v2.0.0 [23]. Genes were clustered using complete linkage with Euclidean distances. The same color scale for gene expression was used for all heatmaps.

2.2.2 Mapping AHBA samples to SCNs of the healthy brain

We focused on anatomical networks that were previously defined based on whole brain gray matter volume covariation in 370 middle-aged to older adults between 45 and 85 years; for more detailed information on the networks see Hafkemeijer et al. 2014. Nine networks were defined and named according to the presence of the main structures: thalamus (network A), lateral occipital cortex (Network B), posterior cingulate cortex (Network C), anterior cingulate cortex (network D), temporal pole (network E), putamen (network F), and cerebellum (networks G, H, and I). The same networks were previously investigated for loss of integrity in 159 PD patients from the same age range; for demographic and clinical information see de Schipper et al. 2017. All samples from each one of the six donors in AHBA were mapped to regions defined by the nine SCNs in MNI coordinate space.

2.2.3 Differential expression analysis

For differential expression analysis we focused on the posterior cingulate network (Network C) and anterior cingulate network (Network D) that were previously associated with gray matter loss in PD [2]. Gene expression in each of the two networks C and D was compared to the other 7 networks together (A, B, E, F, G, H, and I). A two-tailed *t*-test was used for each gene and the analysis was done separately for each donor from AHBA. Since the microarray data was $\log_2$-transformed, the mean expression difference is interpreted as the $\log_2$-transformed fold-change (FC). The effect sizes for each one of the six donors were combined by meta-analysis (metafor R-package 2.0). For the meta-analysis, a random effects model

was applied which assumes that each brain is considered to be from a larger population of brains and therefore takes the within-brain and between-brain variance into account. The between-brain variance (tau^2) was estimated with the Dersimonian-Delaird model. Variances and confidence intervals were obtained using the escalc-function. The significance of summary effect sizes was assessed through a two-sided *t*-test (H_o: FC=0; unequal variances). *P*-values of the effect sizes were Benjamini-Hochberg (BH) corrected for all 20,017 genes. Genes were differentially expressed within the posterior cingulate network or the anterior cingulate network compared to the other networks combined when the absolute fold-change (FC) > 1 and the BH-corrected *P*-value < 0.05.

2.2.4 PATHWAY ANALYSIS

Pathway analysis was done with the ReactomePA R-package version 1.28 using the function *enrichPathway* searching for human pathways. All 20,017 genes in the AHBA dataset were set as background genes. Pathways with a minimum size of 10 genes were significant when the BH-corrected $P < 0.05$.

2.2.5 CELL-TYPE MARKER ENRICHMENT

Gene markers for 28 cell-types were downloaded from the NeuroExpresso database (http://neuroexpresso.org/) using markers from all brain regions. These have been identified in a cross-laboratory dataset of cell-type specific transcriptomes from the mouse brain [24]. To assess their expression, Entrez IDs of the mouse cell-type specific markers were converted to human homologs (homologene R-package version 1.4) and filtered for genes present in the AHBA dataset (Supplementary Table 1). Two markers with different mouse gene IDs (14972, *H2-K1*, microglial, and 15006, *H2-Q1* serotonergic), were converted to the same human gene ID (3105, *HLA-A*), and therefore removed before analysis. For cell-type enrichment, we assessed which cell-type markers were overrepresented among the differentially expressed genes. For 17 cell-types that had at least six markers (astrocyte, Bergmann, cerebellar granule, dentate granule, ependymal, GabaReln, hypocretinergic, microglia, activated microglia, deactivated microglia, noradrenergic, oligo, purkinje, serotonergic, spinal cord cholinergic, spiny, and thalamus cholinergic), we assessed the significance with the hypergeometric test and *P*-values were corrected for all 17 cell-types (BH-corrected $P < 0.05$).

2.2.6 ENRICHMENT OF DISEASE-ASSOCIATED GENES

Differentially expressed genes were also assessed for the overrepresentation of disease-associated genes from DisGeNET [25]. A table of 628,685 gene-disease associations were obtained from DisGeNET version 6.0 (July, 2019) from http://www.disgenet.org/. A hypergeometric test was used to assess the significance of overlapping genes ($P < 0.05$), and *P*-values were BH-corrected for 24,166 diseases. The odds ratio (OR) for cell-type and disease enrichment was calculated using the DescTools R-package.

2.2.7 CODE AVAILABILITY

Scripts to run all analyses can be found online at https://github.com/arlinkeo/pd_scn.

2.3 RESULTS

2.3.1 TRANSCRIPTOMICS OF THE POSTERIOR AND ANTERIOR CINGULATE NETWORKS

We analyzed the transcriptomes of healthy subjects across nine anatomical networks defined by structural covariance of gray matter volume among healthy middle-aged to older adults [21]. For this we used the AHBA microarray dataset of spatial gene expression in post-mortem brains of six non-neurological donors and samples were mapped to each one of the nine networks A-I (Table 2.1) based on their spatial location. We focused on the posterior cingulate network (Network C) and the anterior cingulate network (Network D) that showed loss of gray matter in PD patients (Figure 2.1) [2] and characterized their transcriptional signatures by comparing them to the remaining seven networks together.

Table 2.1 Number of samples from the AHBA that fall within networks A-I.

Donors	Network								
	A	B	C	D	E	F	G	H	I
Donor 9861	72	67	157	47	74	90	26	39	83
Donor 10021	79	46	121	65	49	84	25	55	91
Donor 12876	37	24	57	28	42	45	6	17	25
Donor 14380	38	33	52	30	45	61	7	27	53
Donor 15496	34	24	41	21	39	55	13	24	69
Donor 15697	49	20	38	33	47	64	29	37	49
Total	309	214	466	224	296	399	106	199	370

A: Thalamus; B: Lateral occipital cortex, C: Posterior cingulate cortex, D: Anterior cingulate cortex, E: Temporal pole; F: Putamen; G, H, I: Cerebellum.

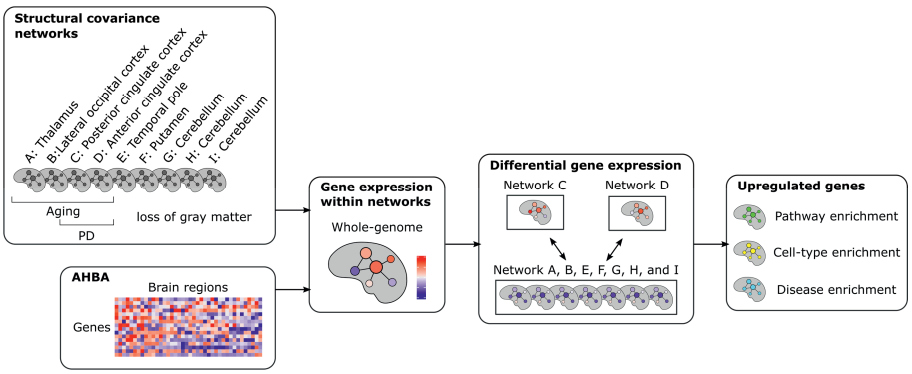

Figure 2.1 Study overview. Transcriptomic data from AHBA were mapped to nine anatomical networks that have been defined based on healthy subjects. The posterior cingulate network (Network C) and anterior cingulate network (Network D) have been associated with gray matter loss in PD, while the seven remaining networks were not related to PD. We compared gene expression in network C and D to gene expression in networks A, B, E, F, G, H, and I together. Upregulated genes were assessed for the overrepresentation of pathway-specific genes, cell-type marker genes, and disease-associated genes.

Whole genome differential expression analysis showed a large overlap of genes that were differentially expressed in the same direction in the two networks. We found that 73 genes in the posterior cingulate network and 39 genes in anterior cingulate network were downregulated, of which 25 genes overlapped between both networks (Figure 2.2AB, Supplementary Table 2 and 3). Furthermore, 200 genes in the posterior cingulate network and 269 genes in anterior cingulate network were upregulated, for which 144 genes overlapped (Supplementary Table 4 and 5). Among the differentially expressed genes in the posterior and anterior cingulate networks, no PD-implicated genes were found that arouse from familial and genome-wide association studies [26–28].

For functional interpretation of the differentially upregulated genes we further assessed their associated pathways (see Methods, Supplementary Table 6). As both networks C and D shared many differentially expressed genes, they also shared similar pathways: transcriptional regulation by *MECP2*, GPCR signaling, voltage gated potassium channels, and neurotransmitter receptor and postsynaptic signal transmission (Figure 2.2C). These pathways are also hierarchically related to each other based on the ontology of the Reactome Pathway Database. The posterior cingulate network was additionally related to more specific pathways such as lysosphingolipid and LPA receptors, GABA receptor activation, RAS-signaling mediated by NMDA receptors, glutamate binding, activation of AMPA receptors and synaptic plasticity, and long-term potentiation. The anterior cingulate cortex was additionally associated with serotonin receptors.

2.3.2 CELL-TYPE ENRICHMENT IN ANATOMICAL NETWORKS

The composition of specific cell-types can shape the transcriptomic features of anatomical networks. Therefore, we analyzed whether genes differentially expressed in the posterior and anterior cingulate networks were enriched for cell-type specific marker genes from the NeuroExpresso database [24]. To assess the expression of each cell-type, we averaged the expression of the marker genes associated with that cell-type. Both the posterior and anterior cingulate networks showed high expression of marker genes for brainstem cholinergic cells, GabaSSTReln, GabaVIPReln, glutamatergic, and pyramidal cells (Figure 2.3 and Supplementary Figure 1).

Among the differentially upregulated genes in the posterior and anterior cingulate networks, we found 10 marker genes representing six cell-types: astrocyte, Bergmann, GabaVIPReln, hypocretinergic, pyramidal, and thalamus cholinergic (Table 2.2). Markers that were significantly upregulated in the posterior cingulate network were also significantly upregulated in the anterior cingulate network. In both networks, the 10 markers were highly expressed in cortical regions, including the cingulate gyrus, and lowly expressed in limbic regions (Figure 2.4 and Supplementary Figure 2).

Only genes upregulated in the anterior cingulate gyrus were significantly enriched for a cell-type, namely thalamus cholinergic cells (OR = 17.12 and P = 2.01e-02). The responsible markers *NPPA*, *SOSTDC1*, and *TYRP1* showed high expression within the anterior cingulate gyrus network, as well as in most parts of the posterior cingulate gyrus network (Figure 2.4).

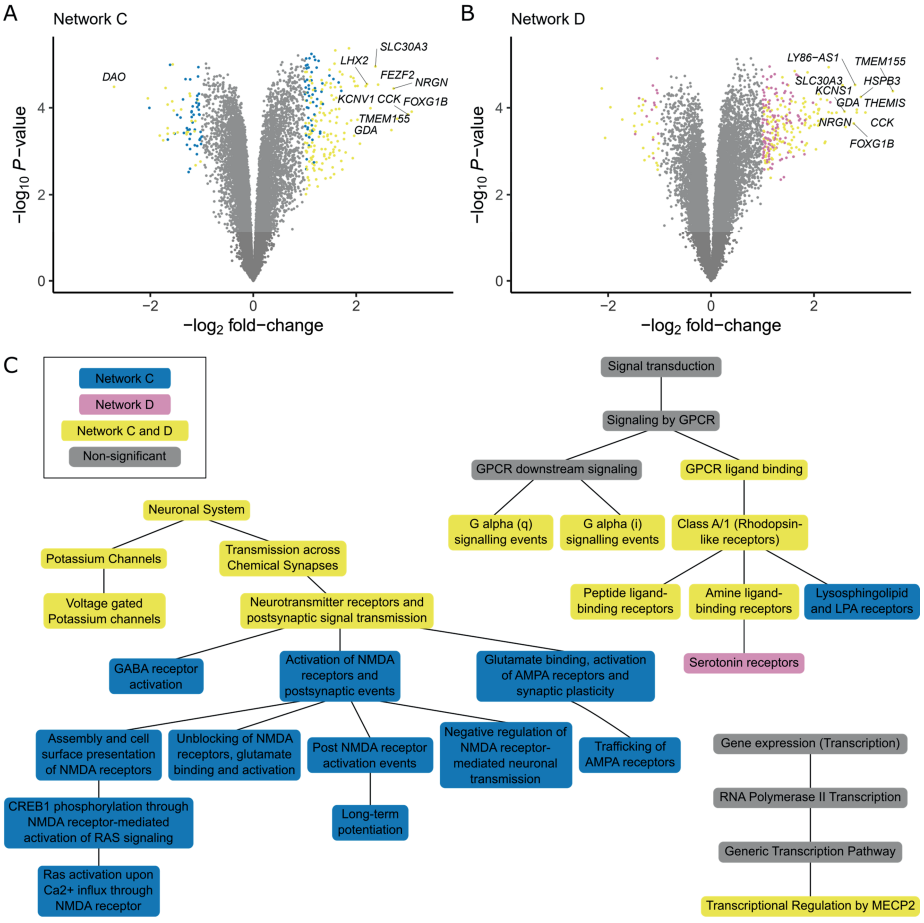

Figure 2.2 Differential expressed genes and associated pathways. Genes were analyzed for differential expression in (A) the posterior cingulate network (Network C) and (B) the anterior cingulate network (Network D). Effect sizes were summarized across the six healthy donors of AHBA with meta-analysis. For all genes (points) the $\log_2$ fold-change (FC; x-axis) and -$\log_{10}$ of nominal *P*-values (y-axis) are shown. Significant differentially expressed genes (*t*-test, BH-corrected $P < 0.05$, and $|FC| > 1$) are unique for each network (blue and purple points) or significant in both networks (yellow points). The top 10 genes with the highest absolute FC are labeled for each network and highly overlap between both networks. (C) Pathway analysis of differentially upregulated genes in the posterior cingulate network and anterior cingulate network. Network C and Network D shared similar pathways (yellow) that are hierarchically organized in the Reactome database. The posterior cingulate network showed more specific associations with pathways involved in neurotransmitter receptors and postsynaptic signal transmission (blue). The anterior cingulate network was more specifically associated with serotonin receptors (purple). See Supplementary Table 6 for gene counts and BH-corrected *P*-values.

Interestingly, while other thalamus cholinergic marker genes showed high expression in limbic samples and low expression in cortical samples within both networks, *NPPA*, *SOSTDC1*, and *TYRP1* showed opposite expression patterns with low expression in limbic samples, including the thalamus, and high expression in cortical samples (Supplementary Figure 3).

Table 2.2 Differentially expressed cell-type marker genes in the posterior cingulate network (Network C) and anterior cingulate network (Network D). Fold-change (FC) and Benjamini-Hochberg (BH) corrected *P*-value are shown for cell-type marker genes that were differentially expressed in the two networks compared to the remaining networks. FC > 1 and BH < 0.05 are highlighted in red text.

Gene	Cell-type	Network C		Network D	
		FC	BH	Estimate	BH
LHX2	Astrocyte	2.21	3.92E-03	2.00	6.46E-03
IGFBP2	Astrocyte	0.69	5.80E-02	1.18	1.78E-02
RORB	Astrocyte	0.82	3.09E-02	1.19	1.39E-02
WIF1	Bergmann	1.02	8.74E-03	1.03	7.95E-03
VIP	GabaVIPReln	1.67	4.23E-03	1.85	6.89E-03
PCSK1	Hypocretinergic	1.15	1.25E-02	1.57	1.06E-02
NEUROD6	Pyramidal	1.90	4.78E-03	1.92	6.76E-03
NPPA	ThalamusCholin	1.64	6.98E-03	2.09	6.39E-03
TYRP1	ThalamusCholin	0.81	2.41E-02	1.43	9.82E-03
SOSTDC1	ThalamusCholin	0.83	1.21E-02	1.14	6.39E-03

Fold-change (FC) and Benjamini-Hochberg (BH) corrected *P*-value for cell-type markers genes that were differentially expressed in network C and D compared to the remaining networks. FC > 1 and BH < 0.05 are highlighted in red.

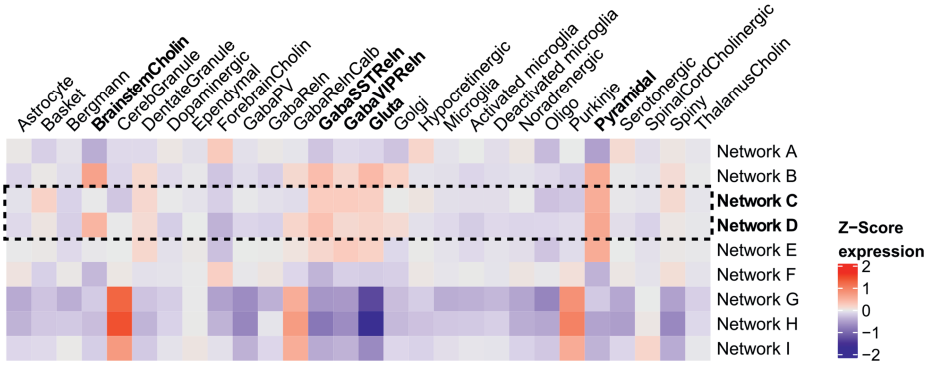

Figure 2.3 Expression of cell-types in anatomical networks. Gene expression was Z-scored and averaged across cell-type specific markers, across samples within anatomical networks, and across the six donors in the AHBA. Networks G, H, and I are cerebellar networks and thus showed distinct expression patterns. The posterior and anterior cingulate networks (Network C and Network D) showed high expression of marker genes for brainstem cholinergic cells, GabaSSTReln, GabaVIPReln, glutamatergic cells, and pyramidal cells. Gene expression heatmaps for each donor are shown in Supplementary Figure 1.

2.3.3 Cingulate networks are enriched for genes associated with cognitive disorders

Dysregulation of functional networks may result in a broader spectrum of disorders than PD. Therefore, we assessed which disease-associated genes from DisGeNET were overrepresented among the differentially upregulated genes in the posterior cingulate network as well as the anterior cingulate network. Since both networks shared many upregulated genes, similar disease-associations were also found. We found that genes upregulated in both networks were significantly associated with epileptic and non-epileptic seizures, many mental disorders (bipolar, panic, autistic, cocaine-related, (age-related) memory, mood, major depressive, and anxiety disorder), pain and schizophrenia (Figure 2.5). The posterior cingulate network was more related to memory and pain-related disorders, while the anterior cingulate network was more related to mental and neuropsychiatric disorders.

2.4 Discussion

The posterior and anterior cingulate networks have been previously associated with decreased gray matter in PD patients. We examined transcriptomic signatures of both networks in the healthy brain to identify molecular mechanisms underlying these two regions. Pathway analysis revealed genes related to gPCR signaling, transcriptional regulation by *MECP2*, and neurotransmitter receptors and postsynaptic signal transmission. We only found significant enrichment of cell-types for genes upregulated in the anterior cingulate gyrus, which were the thalamus cholinergic marker genes. Upon further examination the specific genes were also highly expressed in the posterior cingulate cortex, although not significantly. Moreover, our results showed that both SCNs are associated with multiple neurotransmitter signaling pathways, e.g., serotonin, GPCR, GABA, glutamate, and RAS.

2.4.1 Cholinergic function in PD

Genes that were highly expressed in the anterior cingulate network were significantly enriched for thalamus cholinergic markers, specifically: *NPPA*, *SOSTDC1*, and *TYRP1*. These marker genes, together with other markers of this cell-type, were previously defined based on their expression in cholinergic cells from the mouse thalamus, more specifically the habenula [24]. According to the AHBA ontology the habenula is not part of the thalamus. In this study, most thalamus cholinergic marker genes indeed showed high expression in human thalamic regions. However, *NPPA*, *SOSTDC1*, and *TYRP1* unexpectedly showed opposite expression patterns with mainly high expression in cortical regions and low expression in limbic regions, including the thalamus. Cholinergic circuits are key in cognitive functions and cholinergic denervation of the cortex and thalamus in PD patients may contribute to the transition from PD to PD with dementia [29]. We found that glutamatergic and GABAergic marker genes were also highly expressed within the posterior and anterior cingulate networks, although statistical significance could not be assessed due to the small number of marker genes for these cell-types. Interestingly, acetylcholine release by cholinergic neurons affects glutamatergic and GABAergic signaling by altering the synaptic excitability [30,31]. Moreover, it is thought that dysfunction of cholinergic circuits contributes to cognitive decline associated with neurodegenerative diseases [29].

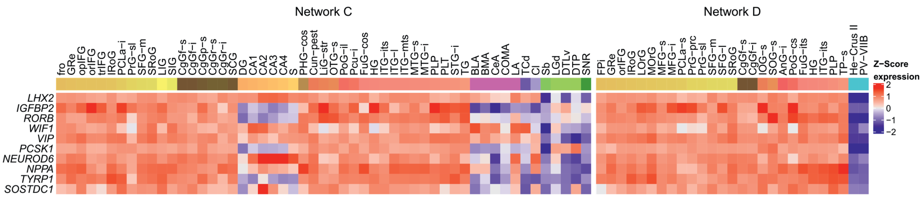

Figure 2.4 Expression of differentially upregulated cell-type marker genes in the posterior cingulate network (Network C) and anterior cingulate network (Network D). Heatmaps of differentially expressed marker genes (rows) are shown for one of the six donors in the Allen Human Brain Atlas (donor 10021). Samples from different anatomical substructures within the networks are color annotated (columns). Expression was averaged across samples from an anatomical substructure with the same acronym ignoring left and right hemisphere annotations. See Supplementary Figure 2 for heatmaps for all six donors from the AHBA and Supplementary Table 7 for full names of the region-specific acronyms.

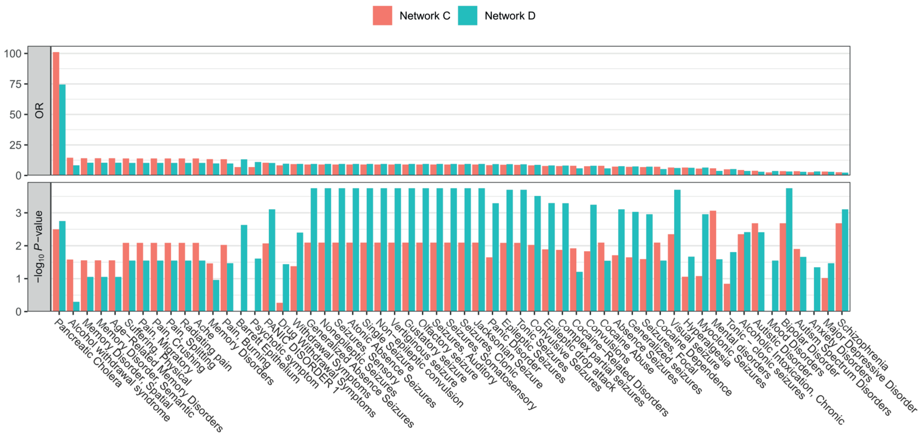

Figure 2.5 Disease associations of the posterior cingulate network (Network C) and anterior cingulate network (Network D). Differentially upregulated genes in each network were assessed for the enrichment of disease-associated genes from DisGeNET (hypergeometric test, BH-corrected $P < 0.05$). Top plot shows odds ratios (ORs) for the number of overlapping genes, and bottom plot shows the significance of overlap indicated with $-\log_{10}$ P-values (y-axis). Disorders (columns) are sorted based on highest ORs in either one of the networks.

2.4.2 *NPPA*, *SOSTDC1*, and *TYRP1*

Cholinergic marker genes *NPPA*, *SOSTDC1*, *TYRP1* were highly expressed in the posterior cingulate network and anterior cingulate network of the healthy brain compared to the other seven SCNs. While the functions of these genes likely involve cholinergic signaling, several studies suggest they also function as extracellular regulators of multiple other signaling pathways, including cAMP, Wnt, and β-catenin signaling [32–37].

NPPA (natriuretic peptide precursor A) and other natriuretic peptides are thought to be involved in a wide range of functions, including neurovascular functions, blood-brain barrier, brain homeostasis, neuroprotection, and synaptic transmission by regulating the release and re-uptake of neurotransmitters such as noradrenalin, dopamine and glycine [38]. Impaired function of natriuretic peptides in brains of AD patients could accelerate neurodegeneration and may impair structural integrity of the brain leading to a higher risk of cognitive decline [39]. Our results suggest that *NPPA* might similarly be involved in PD pathogenesis given its high expression within the anterior and posterior cingulate networks.

SOSTDC1 (sclerostin domain-containing 1) is known as a negative regulator of bone morphogenetic protein (BMP) and Wnt-signaling, but recent studies also show that *SOSTDC1* regulates natural killer cell maturation and cytotoxicity [35]. An increased number of natural killer cells have been found in PD, but the actual relevance with PD risk is still unclear [40]. The BMP signaling pathway promotes the development of midbrain dopaminergic neurons [41], in which *SOSTDC1* may play a role. Furthermore, *SOSTDC1* was upregulated in the striatum of Parkinsonian rats that were treated by subthalamic nucleus high frequency stimulation, and is therefore suggested to have neuroprotective effects [42].

TYRP1 (tyrosinase-related protein 1) produces melanocytes-specific proteins involved in the biosynthesis of melanin in brain, skin and eyes [43,44]. Melanoma and PD share genes involved in the synthesis of melanin and dopamine, including *SNCA* which encodes the α-synuclein protein found in Lewy bodies [45]. Furthermore, neuromelanin is produced almost exclusively in human catecholaminergic neurons and is responsible for the pigmentation of dopaminergic neurons of the substantia nigra, and noradrenergic neurons of the locus cereleus [46]. It is considered to be protective due to its ability to chelate metals, especially iron which increases with age [46].

2.4.3 Disease-associations

The posterior and anterior cingulate networks shared similar highly expressed genes and were likewise associated with similar diseases. Both SCNs represent anatomical networks that function normally in healthy brains, but their activity is reduced in aging and PD [2,21]. As part of the default mode network, both the posterior and anterior cingulate cortex have been shown to be dysregulated in neuropsychiatric disorders [47,48]. Based on our analysis of transcriptomic signatures in the healthy brain, we found that the posterior cingulate network showed stronger associations with memory and pain-related disorders compared to the anterior cingulate networks which showed stronger associations with mental and

neuropsychiatric disorders. Our findings suggest that genes involved in multiple signaling pathways, such as serotonin, GPCR, GABA, glutamate, and RAS, contribute to healthy functions of the posterior and anterior cingulate networks.

2.5 Acknowledgments

We thank L. E. Jonkman for her critical insight on the manuscript. This research received funding from The Netherlands Technology Foundation (STW), as part of the STW project 12721 (Genes in Space). O. Dzyubachyk received funding from The Dutch Research Council (NWO) project 17126 (3DOmics). W. D. J. van de Berg received funding from Alzheimer Netherlands (ISAO #14536) and LECMA (#14797) to study transcriptome datasets in the context of Parkinson's and Alzheimer's disease and was financially supported by grants from Amsterdam Neuroscience; Dutch Research council (ZonMW); Stichting Parkinson Fonds; Alzheimer association; the MJ Fox foundation and Rotary Aalsmeer-Uithoorn. W. D. J. van de Berg performed contract research and consultancy for Hoffmann-La Roche; Lysosomal Therapeutics; CHDR; Cross beta Sciences and received research consumables from Hoffmann-La Roche and Prothena. Prof. J.J. van Hilten received grants from Alkemade-Keuls Foundation; Stichting Parkinson Fonds (Optimist Study); The Netherlands Organisation for Health Research and Development (#40-46000-98-101); NWO (#628.004.001); Hersenstichting; AbbVie; Hoffmann-La-Roche; Lundbeck; and Centre of Human Drug Research outside the submitted work.

References

[1] M. Goedert, M. G. Spillantini, K. Del Tredici, and H. Braak, "100 years of Lewy pathology," *Nat. Rev. Neurol.* 9, 13–24 (2012).

[2] L. J. de Schipper, J. van der Grond, J. Marinus, J. M. L. Henselmans, and J. J. van Hilten, "Loss of integrity and atrophy in cingulate structural covariance networks in Parkinson's disease," *NeuroImage Clin.* 15, 587–593 (2017).

[3] O. Lucas-Jiménez, N. Ojeda, J. Peña, M. Díez-Cirarda, A. Cabrera-Zubizarreta, J. C. Gómez-Esteban, M. Á. Gómez-Beldarrain, and N. Ibarretxe-Bilbao, "Altered functional connectivity in the default mode network is associated with cognitive impairment and brain anatomical changes in Parkinson's disease," *Park. Relat. Disord.* 33, 58–64 (2016).

[4] M. Wang, S. Jiang, Y. Yuan, L. Zhang, J. Ding, J. Wang, J. Zhang, K. Zhang, and J. Wang, "Alterations of functional and structural connectivity of freezing of gait in Parkinson's disease," *J. Neurol.* 263, 1583–1592 (2016).

[5] J. P. M. van der Vegt, B. F. L. van Nuenen, B. R. Bloem, C. Klein, and H. R. Siebner, "Imaging the impact of genes on Parkinson's disease," *Neuroscience* 164, 191–204 (2009).

[6] D. Aarsland, B. Creese, M. Politis, K. R. Chaudhuri, D. H. Ffytche, D. Weintraub, and C. Ballard, "Cognitive decline in Parkinson disease," *Nat. Rev. Neurol.* 13, 217–231 (2017).

[7] F. Sampedro, J. Marín-Lahoz, S. Martínez-Horta, J. Pagonabarraga, and J. Kulisevsky, "Reduced gray matter volume in cognitively preserved COMT ^{158}Val/Val Parkinson's disease patients and its association with cognitive decline," *Brain Imaging Behav.* (2019).

[8] S. E. Winder-Rhodes, A. Hampshire, J. B. Rowe, J. E. Peelle, T. W. Robbins, A. M. Owen, and R. A. Barker, "Association between *MAPT* haplotype and memory function in patients with Parkinson's disease and healthy aging individuals," *Neurobiol. Aging* 36, 1519–1528 (2015).

[9] A. Arnatkevičiūtė, B. D. Fulcher, and A. Fornito, "A practical guide to linking brain-wide gene expression and neuroimaging data," *Neuroimage* 189, 353–367 (2019).

[10] M. Hawrylycz, J. A. Miller, V. Menon, D. Feng, T. Dolbeare, A. L. Guillozet-Bongaarts, A. G. Jegga, B. J. Aronow, C.-K. K. Lee, et al., "Canonical genetic signatures of the adult human brain," *Nat. Neurosci.* 18, 1832–1844 (2015).

[11] B. S. Freeze, D. Acosta, S. Pandya, Y. Zhao, and A. Raj, "Regional expression of genes mediating trans-synaptic alpha-synuclein transfer predicts regional atrophy in Parkinson disease," *NeuroImage Clin.* 18, 456–466 (2018).

[12] T. Rittman, M. Rubinov, P. E. Vértes, A. X. Patel, C. E. Ginestet, B. C. P. Ghosh, R. A. Barker, M. G. Spillantini, E. T. Bullmore, et al., "Regional expression of the *MAPT* gene is associated with loss of hubs in brain networks and cognitive impairment in Parkinson disease and progressive supranuclear palsy," *Neurobiol. Aging* 48, 153–160 (2016).

[13] A. Alexander-Bloch, J. N. Giedd, and E. Bullmore, "Imaging structural co-variance between human brain regions," *Nat. Rev. Neurosci.* 14, 322–336 (2013).

[14] E. M. Coppen, J. van der Grond, A. Hafkemeijer, S. A. R. B. Rombouts, and R. A. C. Roos, "Early grey matter changes in structural covariance networks in Huntington's disease," *NeuroImage Clin.* 12, 806–814 (2016).

[15] C. W. Huang, S. W. Hsu, S. J. Tsai, N. C. Chen, M. E. Liu, C. C. Lee, S. H. Huang, W. N. Chang, Y. T. Chang, et al., "Genetic effect of interleukin-1 beta (C-511T) polymorphism on the structural covariance network and white matter integrity in Alzheimer's disease," *J. Neuroinflammation* 14, 1–13 (2017).

[16] R. N. Spreng and G. R. Turner, "Structural Covariance of the Default Network in Healthy and Pathological Aging," *J. Neurosci.* 33, 15226–15234 (2013).

[17] A. Alexander-Bloch, A. Raznahan, E. Bullmore, and J. Giedd, "The convergence of maturational change and structural covariance in human cortical networks," *J. Neurosci.* 33, 2889–2899 (2013).

[18] F. Liu, H. Tian, J. Li, S. Li, and C. Zhuo, "Altered voxel-wise gray matter structural brain networks in schizophrenia: Association with brain genetic expression pattern," *Brain Imaging Behav.* 13, 493–502 (2019).

[19] Y. Yee, D. J. Fernandes, L. French, J. Ellegood, L. S. Cahill, D. A. Vousden, L. Spencer Noakes, J. Scholz, M. C. van Eede, et al., "Structural covariance of brain region volumes is associated with both structural connectivity and transcriptomic similarity," *Neuroimage* 179, 357–372 (2018).

[20] R. Romero-Garcia, K. J. Whitaker, F. Váša, J. Seidlitz, M. Shinn, P. Fonagy, R. J. Dolan, P. B. Jones, I. M. Goodyer, et al., "Structural covariance networks are coupled to expression of genes enriched in supragranular layers of the human cortex," *Neuroimage* 171, 256–267 (2018).

[21] A. Hafkemeijer, I. Altmann-schneider, A. J. M. De Craen, P. E. Slagboom, J. van der Grond, and S. A. R. B. Rombouts, "Associations between age and gray matter volume in anatomical brain networks in middle-aged to older adults," *Aging Cell* 13, 1068–1074 (2014).

[22] P. Langfelder and S. Horvath, "WGCNA: an R package for weighted correlation network analysis," *BMC Bioinformatics* 9, 1–13 (2008).

[23] Z. Gu, R. Eils, and M. Schlesner, "Complex heatmaps reveal patterns and correlations in multidimensional genomic data," 2847–2849 (2016).

[24] B. O. Mancarci, L. Toker, S. J. Tripathy, B. Li, B. Rocco, E. Sibille, and P. Pavlidis, "Cross-Laboratory Analysis of Brain Cell Type Transcriptomes with Applications to Interpretation of Bulk Tissue Data," *eNeuro* 4, 1–20 (2017).

[25] J. Piñero, À. Bravo, N. Queralt-Rosinach, A. Gutiérrez-Sacristán, J. Deu-Pons, E. Centeno, J. García-García, F. Sanz, and L. I. Furlong, "DisGeNET: A comprehensive platform integrating information on human disease-associated genes and variants," *Nucleic Acids Res.* 45, D833–D839 (2017).

[26] V. Bonifati, "Genetics of Parkinson's disease – state of the art, 2013," *Parkinsonism Relat.*

Disord. 20, S23–S28 (2014).

[27] M. A. Nalls, N. Pankratz, C. M. Lill, C. B. Do, D. G. Hernandez, M. Saad, A. L. Destefano, E. Kara, J. Bras, et al., "Large-scale meta-analysis of genome-wide association data identifies six new risk loci for Parkinson's disease," *Nat. Publ. Gr.* 46, 989–993 (2014).

[28] D. Chang, M. A. Nalls, I. B. Hallgrímsdóttir, J. Hunkapiller, M. van der Brug, F. Cai, G. A. Kerchner, G. Ayalon, B. Bingol, et al., "A meta-analysis of genome-wide association studies identifies 17 new Parkinson's disease risk loci," *Nat. Genet.* 49, 1511–1516 (2017).

[29] E. C. Ballinger, M. Ananth, D. A. Talmage, and L. W. Role, "Basal forebrain cholinergic circuits and signaling in cognition and cognitive Decline," *Neuron* 91, 1199–1218 (2016).

[30] A. J. Granger, N. Mulder, A. Saunders, and B. L. Sabatini, "Cotransmission of acetylcholine and GABA," *Neuropharmacology* 100, 40–46 (2015).

[31] J. J. D. Buendia, L. Tiroshi, W. Chiu, and J. A. Goldberg, "Selective remodeling of glutamatergic transmission to striatal cholinergic interneurons after dopamine depletion," *Eur. J. Neurosci.* 49, 824–833 (2019).

[32] M. K. Kutchko and J. Siltberg-Liberles, "Metazoan innovation : from aromatic amino acids to extracellular signaling," *Amino Acids* 45, 359–367 (2013).

[33] Y. Bansho, J. Lee, E. Nishida, and M. Nakajima-Koyama, "Identification and characterization of secreted factors that are upregulated during somatic cell reprogramming," *FEBS Lett.* 591, 1584–1600 (2017).

[34] B. M. Brenner, B. J. Ballermann, M. E. Gunning, and M. L. Zeidel, "Diverse biological actions of atrial natriuretic peptide," *Physiol. Rev.* 70, 665–699 (1990).

[35] A. J. Millan, S. R. Elizaldi, E. M. Lee, J. O. Aceves, D. Murugesh, G. G. Loots, and J. O. Manilay, "Sostdc1 regulates NK cell maturation and cytotoxicity," *J. Immunol.* 202, 2296–2306 (2019).

[36] P. De Vito, "Atrial natriuretic peptide: An old hormone or a new cytokine?," *Peptides* 58, 108–116 (2014).

[37] T. Hirobe, "How are proliferation and differentiation of melanocytes regulated?," *Pigment Cell Melanoma Res.* 24, 462–478 (2011).

[38] S. Mahinrad, A. J. M. de Craen, S. Yasar, D. van Heemst, and B. Sabayan, "Natriuretic peptides in the central nervous system: Novel targets for cognitive impairment," *Neurosci. Biobehav. Rev.* 68, 148–156 (2016).

[39] S. Mahinrad, M. Bulk, I. van der Velpen, A. Mahfouz, W. van Roon-Mom, N. Fedarko, S. Yasar, B. Sabayan, D. van Heemst, et al., "Natriuretic peptides in post-mortem brain tissue and cerebrospinal fluid of non-demented humans and Alzheimer's disease patients," *Front. Neurosci.* 12, 1–12 (2018).

[40] S. Jiang, H. Gao, Q. Luo, P. Wang, and X. Yang, "The correlation of lymphocyte subsets, natural killer cell, and Parkinson's disease: a meta-analysis," *Neurol. Sci.* 38, 1373–1380 (2017).

[41] V. M. Jovanovic, A. Salti, H. Tilleman, K. Zega, M. M. Jukic, H. Zou, R. H. Friedel, N. Prakash, S. Blaess, et al., "BMP/SMAD pathway promotes neurogenesis of midbrain dopaminergic neurons in vivo and in human induced pluripotent and neural stem cells," *J. Neurosci.* 38, 1662–1676 (2018).

[42] S. Lortet, E. Lacombe, N. Boulanger, P. Rihet, C. Nguyen, L. K. Le Goff, and P. Salin, "Striatal Molecular Signature of Subchronic Subthalamic Nucleus High Frequency Stimulation in Parkinsonian Rat," *PLoS One* 8, e60447 (2013).

[43] N. Wang and D. N. Hebert, "Tyrosinase maturation through the mammalian secretory pathway: Bringing color to life," *Pigment Cell Res.* 19, 3–18 (2006).

[44] H. Lu, L. Li, E. R. Watson, R. W. Williams, E. E. Geisert, M. M. Jablonski, and L. Lu, "Complex interactions of Tyrp1 in the eye.," *Mol. Vis.* 17, 2455–2468 (2011).

[45] T. Pan, J. Zhu, W. J. Hwu, and J. Jankovic, "The role of alpha-synuclein in melanin synthesis

in melanoma and dopaminergic neuronal cells," *PLoS One* 7, 3–10 (2012).

[46] B. Pavan and A. Dalpiaz, "Odorants could elicit repair processes in melanized neuronal and skin cells," *Neural Regen. Res.* 12, 1401–1404 (2017).

[47] D. Öngür, M. Lundy, I. Greenhouse, A. K. Shinn, V. Menon, B. M. Cohen, and P. F. Renshaw, "Default mode network abnormalities in bipolar disorder and schizophrenia," *Psychiatry Res. - Neuroimaging* 183, 59–68 (2010).

[48] S. J. Broyd, C. Demanuele, S. Debener, S. K. Helps, C. J. James, and E. J. S. Sonuga-Barke, "Default-mode brain dysfunction in mental disorders: A systematic review," *Neurosci. Biobehav. Rev.* 33, 279–296 (2009).